HHS Public Access

Author manuscript

Ann Thorac Surg. Author manuscript; available in PMC 2019 August 07.

Published in final edited form as:

Ann Thorac Surg. 2017 April ; 103(4): 1171–1177. doi:10.1016/j.athoracsur.2016.11.083.

Regional Heterogeneity in the Mitral Valve Apparatus in Patients With Ischemic Mitral Regurgitation

Feroze Mahmood, MD, **Ziyad O. Knio, BS**, **Lu Yeh, MD**, **Rabia Amir, MD**, **Robina Matyal, MD**, **Azad Mashari, MD**, **Robert C. Gorman, MD**, **Joseph H. Gorman III, MD**, **Kamal R. Khabbaz, MD**

Departments of Anesthesia, Critical Care and Pain Medicine and Surgery, Division of Cardiac Surgery, Beth Israel Deaconess Medical Center, Harvard Medical School, Boston, Massachusetts; Department of Anesthesia and Pain Medicine, University of Groningen, University Medical Center, Groningen, Netherlands; Department of Anesthesia and Pain Management, Toronto General Hospital, University Health Network, University of Toronto, Toronto, Ontario, Canada; and Department of Surgery, University of Pennsylvania, Philadelphia, Pennsylvania

Abstract

Background—Apical displacement of the coaptation point of the mitral valve (MV) in response to ischemic mitral regurgitation (IMR) represents remodeling of the MV apparatus. Whereas it implies chronicity, it lacks specificity in discriminating normal from a significantly remodeled MV apparatus. Regional aspects of MV remodeling have shown superior value over global remodeling in predicting recurrence after MV repair for IMR. Quite possibly, presence of specific regional changes in MV geometry that are unique to chronic IMR patients could also be used to diagnose the presence and track progression of remodeling. Knowledge of these changes in MV apparatus in patients with IMR can possibly be used to identify patients for surgical intervention before irreversible remodeling occurs.

Methods—Three-dimensional transesophageal echocardiographic data were collected from patients who underwent MV surgery for IMR (IMR group, n = 66), and from patients with normal valvular and biventricular function (control group, n = 10). The acquired data of the MV were geometrically analyzed to make regional comparisons between the IMR and the control group to identify measurements that reliably differentiate normal from remodeled MVs.

Results—Lengthening of the middle potion of the anterior annulus (A2 regional perimeter: 11.149 mm versus 9.798 mm, $p = 0.0041$), larger nonplanarity angle (147.985 versus 140.720 degrees, $p = 0.0459$), and increased tenting angle of the posteromedial scallop of the posterior leaflet (P3 tenting angle: 44.354 versus 40.461 degrees, $p = 0.0435$) were sufficient in differentiating between IMR and the control group.

Address correspondence to Dr Khabbaz, Department of Surgery, Division of Cardiac Surgery, Beth Israel Deaconess Medical Center, Harvard Medical School, 1 Deaconess Rd, CC454, Boston, MA 02215; kkhabbaz@bidmc.harvard.edu.

The authors had full control of the design of the study, methods used, outcome parameters and results, analysis of data, and production of the written report.

The Video can be viewed in the online version of this article [http://dx.doi.org/10.1016/j.athoracsur.2016.11.083] on http://www.annalsthoracicsurgery.org.

Conclusions—Specific three-dimensional changes in MV geometry can be used to reliably identify a significantly remodeled valve apparatus.

Ischemic mitral regurgitation (IMR) is a challenging clinical condition with considerable debate regarding the optimal therapy. In addition to the clinical context, chronicity and severity of mitral regurgitation (MR), and likelihood of recurrence are considered during surgical decision-making. Whereas mitral valve (MV) repair has certain advantages over replacement [1–3], it is associated with a higher rate of recurrent MR after repair [1, 2, 4–6]. Therefore, recommendations based on these data favor MV replacement over repair for IMR. Interestingly, patients who undergo MV repair and do not have recurrent MR have significantly better postoperative functional status than patients who had recurrent MR [1]. Possibly, the MV apparatus of those with recurrent MR after MV repair had irreversibly remodeled, and predictably, no benefit was derived from repair. Therefore, optimal timing of IMR surgery and selecting patients before irreversible remodeling would be clinically beneficial.

Apical displacement of the coaptation point is considered a sign of chronicity of MR and significant valvular remodeling. It is a global measure and lacks discriminatory value in differentiating normal from a remodeled MV as result of chronic IMR. Recent studies have demonstrated that regional geometric distortions in the mitral valve apparatus (eg, restriction of the posteromedial scallop of the posterior leaflet [P3 region]) could possibly be used to predict the likelihood of recurrence of MR after MV repair [4, 7]. Regional restrictions of leaflet motion are the endpoint of localized remodeling of MV apparatus. There could possibly be other changes in the architecture of the MV apparatus that predispose this regional leaflet restriction. Knowledge and description of these specific regional differences in MV geometry between normal MVs and those with IMR can be clinically useful in addressing the pathophysiology and in selecting the timing and the nature of most suitable intervention.

In this study, we describe the three-dimensional (3D) conformation of the MV by virtual reconstruction from 3D echocardiographic data and by quantifying regional measurements of geometry with precision. These regional measures were then compared between patients with IMR who underwent MV repair/replacement and patients with normal MV function at our medical center to identify the discriminating structural alterations in patients with IMR.

Patients and Methods

This study was conducted as part of an ongoing Institutional Review Board-approved protocol for intraoperative three-dimensional transesophageal echocardiographic (3D-TEE) data collection with waiver of informed consent. For the purpose of this study, data of only patients who underwent elective cardiac surgery with intraoperative 3D-TEE were included. The IMR group consisted of patients undergoing elective coronary artery bypass grafting and MV repair/replacement at our institution between 2008 and 2016. In the IMR group, any degenerative component in the MV (prolapse, flail, perforation), stenosis, or any other valvular abnormality (aortic stenosis, tricuspid regurgitation) were considered to be exclusionary criteria. The control group consisted of patients undergoing coronary artery

bypass graft surgery at our institution with normal intracardiac chamber dimensions, biventricular systolic function, and valvular function. The IMR MVs and control group MVs were geometrically analyzed and compared.

Equipment and Imaging Protocol

All echocardiographic data were collected after induction of general anesthesia, and before sternotomy and institution of cardiopulmonary bypass. A comprehensive two-dimensional TEE examination was performed, followed by a focused 3D-TEE examination. Images were acquired through a mid esophageal four-chamber view using the Philips iE-33 Ultrasound System with an X7–2t TEE probe (Phillips Healthcare, Andover, MA). The 3D-TEE imaging protocol has been described previously [8]. Briefly, imaging of the MV was initiated in the mid esophageal four-chamber window to include the entire mitral annulus leaflets and the coaptation point in the region of interest. The R-wave gated imaging of the MV was initiated during a brief period of apnea and lack of patient movement. For patients with irregular rhythm, a single-beat, wide-angle mode was used for image acquisition. Acquired images were immediately assessed by the 3D quantification software for quality and lack of imaging artifacts. Satisfactory data were then exported to a USB drive in the digital imaging for communication in medicine (DICOM) format for offline analysis.

Assessment of Regurgitation Severity

Intraoperative severity of MR was assessed with the vena contracta method [9]. The vena contracta width was measured in the mid esophageal four-chamber view with color flow Doppler and using the zoom mode to measure the narrowest portion of the MR jet (Fig 1) [4].

Virtual Reconstruction and Regional Analysis

All acquired data were analyzed using the Image Arena Software (TomTec Imaging Systems GmBH, Munich, Germany). Within the environment of the Image Arena, 4D MV Assessment Version 2 software was launched for further semiautomated analysis. The process started with identification of end diastole as the first frame with MV closure and end systole as the last frame before the MV started to open. The mid systole frame number was defined as the median of the end diastole frame number and the end systole frame number. In mid systole, the MV annulus was manually marked in anteroposterior and anterolateral-posteromedial dimensions, and the apical aortic annulus point was identified. Based on these temporal and spatial landmarks, annular dimensions and a digital leaflet topographical surface data were generated. For each MV analysis, a .mat file containing a triangular surface mesh for each systolic frame was exported from the software for further geometric analysis. Each mesh consisted of 1,600 Cartesian coordinates defining annular and commissural points, and discriminating between anterior and posterior surface triangles of the leaflet surface. The .mat file was imported to R software (R Core Group, Vienna, Austria) for virtual reconstruction and regional analysis.

The R software was used to plot each valve in 3D space (Fig 2, Video), and global and regional measurements were computed using the Cartesian coordinates of the valve’s points. Carpentier’s classification of MV nomenclature was used to describe MV anatomy [10,11].

Measurements that were obtained included anteroposterior and anterolateral-posteromedial diameters, tenting height, regional and global perimeters, regional and global leaflet areas, commissure width and path length, regional and global tenting volumes, nonplanarity angle, and regional tenting angles (Table 1).

Statistical Analysis

Student's *t* test was used to compare means of each of the global and regional parameters between the IMR group and the control group at mid systole. A significance level of 0.05 was used to identify factors that differed significantly between the two groups. These factors were entered as potential predictors into a bidirectional stepwise logistic regression model using the Akaike information criterion cutoff for inclusion, defining diagnosis (IMR versus control) as the binary response. The R software accomplishes this by algorithmically adding and removing predictors until the model fit (measured by the Akaike information criterion) can no longer be improved with additional iterations. The predictors of IMR in the final regression model were considered nonredundant informative regional measures that are sufficient in predicting incidence of MR and therefore indicative of MV remodeling. The model's calibration and discrimination were evaluated with a Hosmer-Lemeshow hypothesis test and a c-statistic, respectively.

Results

In all, 76 patients undergoing cardiac procedures between 2008 and 2016 were included in the study. Of these 76 patients, 66 patients were undergoing MV procedures for IMR (IMR group) and 10 had normal valvular and biventricular function (control group). The patients with IMR were older, had greater body mass index, and had poorer left ventricular ejection fractions than patients without MR (Table 2).

Regional measurements that differed between the IMR group and the control group at a 0.05 significance level were as follows: anteroposterior diameter, A2 regional perimeter, anterior perimeter, A1 regional leaflet area, A3 regional leaflet area, anterior leaflet area, A3 regional tenting volume, nonplanarity angle, and P3 tenting angle (Table 3). The values for each of these measurements indicated that MVs with IMR were generally dilated and more tethered than normal MVs (Table 3). Many of these measurements exhibited strong correlations with each other (Fig 3), which supported the need for model selection.

Applying the model selection criterion showed that a valve could be diagnosed using only the A2 regional perimeter, nonplanarity angle, and P3 tenting angle (Fig 4, Table 4). More specifically, patients with IMR exhibited annular lengthening in A2 region, increased nonplanarity angle, and increased tethering in P3 region as compared with patients with normal MVs. A Hosmer-Lemeshow hypothesis test showed that the model was well calibrated ($p = 0.636$), and a c-statistic calculation showed that the model had very strong discriminative ability (c = 0.787).

Comment

In this study, we have demonstrated that there are numerous geometric differences in the MV apparatus of patients with IMR as compared with patients having normal MVs. Differences in regional MV structure and function have been described in previous studies [4,6,12–14]. Our results have identified additional specific structural parameters that can reliably identify an MV apparatus that has undergone significant remodeling. Specifically, annular lengthening in the A2 region, increased nonplanarity angle, and increased tenting in P3 region are indicative of IMR related remodeling. These geometric alterations reliably differentiated the two groups in our study. Our results support and add to the previously demonstrated regional distortions in MV geometry in patients with IMR [14–16]. In this study, the IMR group consisted of patients who underwent surgical intervention for IMR and therefore had significant MV apparatus remodeling. The results are also significant in that they can be used to quantify the extent and track the progression of remodeling of the MV apparatus by performing serial echocardiograms. This methodology may be applied longitudinally to track MV remodeling, with a focus on the identified structural deformations. That would allow for comparison of outcomes such as worsening MR grade or recurrent MR after surgery between patients managed conservatively and those undergoing surgical therapy. It is possible that such an investigation would suggest that the three identified deformations can be used in deciding the timing of surgery in patients with IMR.

Global MA dilation and apical displacement of the coaptation point have traditionally been considered the hallmarks of chronic remodeling requiring therapy [3,17,18]. These global measures, however, do not describe the regional heterogeneity of the MV apparatus in response to ischemia. Ischemic remodeling variably affects various components (ventricular, annular, leaflet) of the MV apparatus [13,19,20]. Significant regional remodeling in IMR patients is a predictor of recurrence after surgical MV repair [4, 7]. Based on the extent of remodeling, appropriate patient selection for MV repair can possibly reduce the incidence of recurrent MR and improve functional recovery [4]. Our study has demonstrated lengthening of A2 regional perimeter, increased nonplanarity angle, and increased tenting in the P3 region as additional differentiating features between normal and IMR patients. Lengthening of annular perimeter in the A2 region, which is normally considered a fibrous/rigid portion, implies significant annular distortion. Indeed, it is apparent that lengthening of annular perimeter in the A2 region is strongly correlated with additional annular distortions, such as lengthening of annular perimeter in posterior regions and greater annular area (Fig 3). Similarly, an increased nonplanarity angle implies significant flattening of the saddle shape of the mitral annulus [2,15,16,21,22].

Traditional geometric analyses of the mitral valve have been based on global measures alone [19], and reconstructions from limited spatial points in the 3D space [23]. Moreover, some methodologies require forcibly fitting the mitral annulus to a planar surface [24]. In addition, correlations between regional measures of annular conformation have not been investigated with a degree of precision [25]. Using our methodology, reconstructing the entire MV from 1,600 spatial points allowed us to obtain more robust global and regional measures about the geometry of the MV. The superior spatial resolution also enabled us to appreciate the

nonplanar geometry of the MA without making geometric assumptions. Moreover, rather than identifying all regional anatomical differences between healthy MVs and IMR MVs, we reduced the outcomes to three nonredundant informative regional measures that are sufficient in describing remodeling. It is also worth noting that although numerous global measurements were considered, no such measures differed between the two groups, supporting the hypothesis that regional distortions, rather than global distortions alone, should be considered when evaluating therapies. Nonplanarity angle and annular dimensions can be measured in a clinically feasible fashion and possibly incorporated into clinical decision making. Most commercially available 3D analytical software have the capability of making these assessments. Therefore, the impact of our findings can be evaluated during routine clinical assessment.

We can identify a few limitations of the study. First, we do not have the outcome data regarding recurrence of MR after repair in this patient cohort. However, the current study was not focused on outcome, but rather on the heterogeneity of MV architecture in patients with IMR. Second, our analyses were performed retrospectively and would need validation in a prospective study. However, our study confirmed the presence of some changes in mitral annular geometry that have been demonstrated in previous reports [4, 7, 15, 17, 23]. Therefore, we are confident in the validity of our finding. Although the size of the control group is somewhat limited, the variance of the 10 control valves is similar to the variance of the 66 diseased valves (Table 3), suggesting that increasing the sample size would not significantly alter the results.

In conclusion, our study has demonstrated significant changes in MV apparatus geometry in patients with IMR as compared with patients having normal valvular and biventricular function. These regional geometric changes can be used to identify significant MV apparatus remodeling that may warrant intervention.

Supplementary Material

Refer to Web version on PubMed Central for supplementary material.

References

1. Acker MA, Parides MK, Perrault LP, et al. Mitral-valve repair versus replacement for severe ischemic mitral regurgitation. N Engl J Med 2014;370:23–32. [PubMed: 24245543]
2. Bouma W, Aoki C, Vergnat M, et al. Saddle-shaped annu-loplasty improves leaflet coaptation in repair for ischemic mitral regurgitation. Ann Thorac Surg 2015;100:1360–6. [PubMed: 26184554]
3. La Piérard, Carabello BA. Ischaemic mitral regurgitation: pathophysiology, outcomes and the conundrum of treatment. Eur Heart J 2010;31:2996–3005. [PubMed: 21123277]
4. Bouma W, Lai EK, Levack MM, et al. Preoperative three-dimensional valve analysis predicts recurrent ischemic mitral regurgitation after mitral annuloplasty. Ann Thorac Surg 2016;101:567–75. [PubMed: 26688087]
5. Kuwahara E, Otsuji Y, Iguro Y, et al. Mechanism of recur-rent/persistent ischemic/functional mitral regurgitation in the chronic phase after surgical annuloplasty: importance of augmented posterior leaflet tethering. Circulation 2006;114: I529–34. [PubMed: 16820632]
6. Fino C, Iacovoni A, Ferrero P, et al. Determinants of functional capacity after mitral valve annuloplasty or replacement for ischemic mitral regurgitation. J Thorac Cardiovasc Surg 2015;149:1595–603. [PubMed: 25886713]

7. Ciarka A, Braun J, Delgado V, et al. Predictors of mitral regurgitation recurrence in patients with heart failure undergoing mitral valve annuloplasty. Am J Cardiol 2010;106: 395–401. [PubMed: 20643253]
8. Mahmood F, Jeganathan J, Saraf R, et al. A practical approach to an intraoperative three-dimensional transesophageal echocardiography examination. J Cardiothorac Vasc Anesth 2016;30:470–90. [PubMed: 26792655]
9. Miyatake K, Izumi S, Okamoto M, et al. Semiquantitative grading of severity of mitral regurgitation by real-time twodimensional Doppler flow imaging technique. J Am Coll Cardiol 1986;7:82–8. [PubMed: 3941221]
10. Carpentier AF, Lessana A, Relland JY, et al. The "physioring": an advanced concept in mitral valve annuloplasty. Ann Thorac Surg 1995;60:1177–86. [PubMed: 8526596]
11. Carpentier A Cardiac valve surgery—the "French correction." J Thorac Cardiovasc Surg 1983;86:323–37. [PubMed: 6887954]
12. Shakil O, Jainandunsing JS, Ilic R, Matyal R, Mahmood F. Ischemic mitral regurgitation: an intraoperative echocardio- graphic perspective. J Cardiothorac Vasc Anesth 2013;27:573–85. [PubMed: 22819468]
13. Silbiger JJ. Mechanistic insights into ischemic mitral regurgitation: echocardiographic and surgical implications. J Am Soc Echocardiogr 2011;24:707–19. [PubMed: 21592725]
14. Kwan J, Shiota T, Agler DA, et al. Geometric differences of the mitral apparatus between ischemic and dilated cardiomyopathy with significant mitral regurgitation: real-time three-dimensional echocardiography study. Circulation 2003;107:1135–40. [PubMed: 12615791]
15. Gorman JH, Jackson BM, Enomoto Y, Gorman RC. The effect of regional ischemia on mitral valve annular saddle shape. Ann Thorac Surg 2004;77:544–8. [PubMed: 14759435]
16. Daimon M, Saracino G, Fukuda S, et al. Dynamic change of mitral annular geometry and motion in ischemic mitral regurgitation assessed by a computerized 3D echo method. Echocardiography 2010;27:1069–77. [PubMed: 20546009]
17. Khabbaz KR, Mahmood F, Shakil O, et al. Dynamic 3-dimensional echocardiographic assessment of mitral annular geometry in patients with functional mitral regurgitation. Ann Thorac Surg 2013;95:105–10. [PubMed: 23103005]
18. Chaput M, Handschumacher MD, Guerrero JL, et al. Mitral leaflet adaptation to ventricular remodeling: prospective changes in a model of ischemic mitral regurgitation. Circulation 2009;120:S99–103. [PubMed: 19752393]
19. Magne J, Pibarot P, Dumesnil JG, Sénéchal M. Continued global left ventricular remodeling is not the sole mechanism responsible for the late recurrence of ischemic mitral regurgitation after restrictive annuloplasty. J Am Soc Echocardiogr 2009;22:1256–64. [PubMed: 19815380]
20. Agricola E, Oppizzi M, Pisani M, Meris A, Maisano F, Margonato A. Ischemic mitral regurgitation: mechanisms and echocardiographic classification. Eur J Echocardiogr 2008;9: 207–21. [PubMed: 17600766]
21. Jensen MO, Jensen H, Levine RA, et al. Saddle-shaped mitral valve annuloplasty rings improve leaflet coaptation geometry. J Thorac Cardiovasc Surg 2011;142:697–703. [PubMed: 21329946]
22. Tibayan FA, Rodriguez F, Langer F, et al. Annular remodeling in chronic ischemic mitral regurgitation: ring selection implications. Ann Thorac Surg 2003;76:1549–55. [PubMed: 14602284]
23. Little SH, Ben Zekry S, Lawrie GM, Zoghbi WA. Dynamic annular geometry and function in patients with mitral regurgitation: insight from three-dimensional annular tracking. J Am Soc Echocardiogr 2010;23:872–9. [PubMed: 20659666]
24. Ormiston JA, Shah PM, Tei C, Wong M. Size and motion of the mitral valve annulus in man. I. A two-dimensional echocardiographic method and findings in normal subjects. Circulation 1981;64:113–20. [PubMed: 7237707]
25. Ryan LP, Jackson BM, Enomoto Y, et al. Description of regional mitral annular nonplanarity in healthy human subjects: a novel methodology. J Thorac Cardiovasc Surg 2007;134:644–8. [PubMed: 17723812]

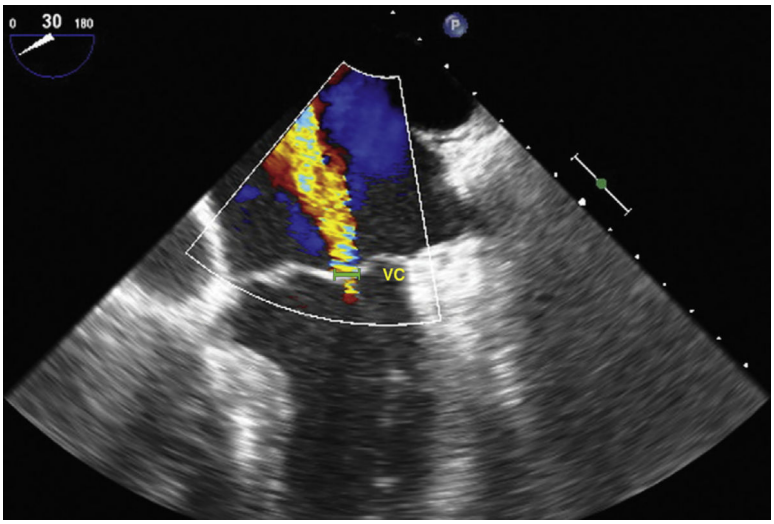

Fig 1.

Mid esophageal four-chamber view of a regurgitant mitral valve, utilizing the vena contracta (VC) method to grade the severity of mitral regurgitation.

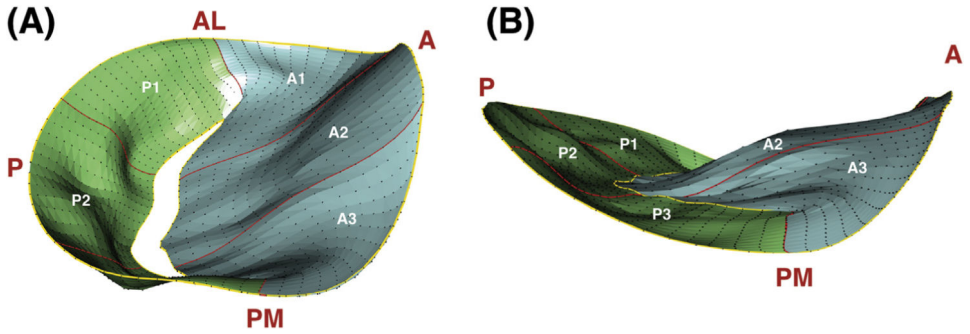

Fig 2.

Three-dimensional reconstruction of (A) ischemic and (B) normal mitral valves at mid systole, with anteroposterior and anterolateral-posteromedial points marked. Regions are also identified. (A = anterior, AL = anterolateral; P = posterior, PM = posteromedial.)

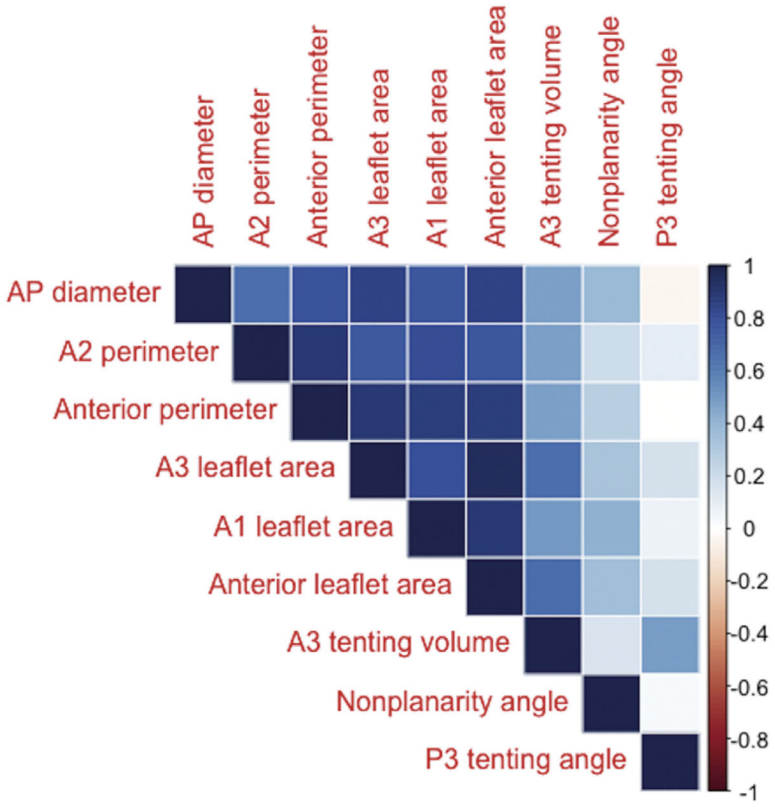

Fig 3.

Correlation plots describing the collinearity of regional measurements that differed between ischemic regurgitant valves and normal mitral valves. (AP = anteroposterior.)

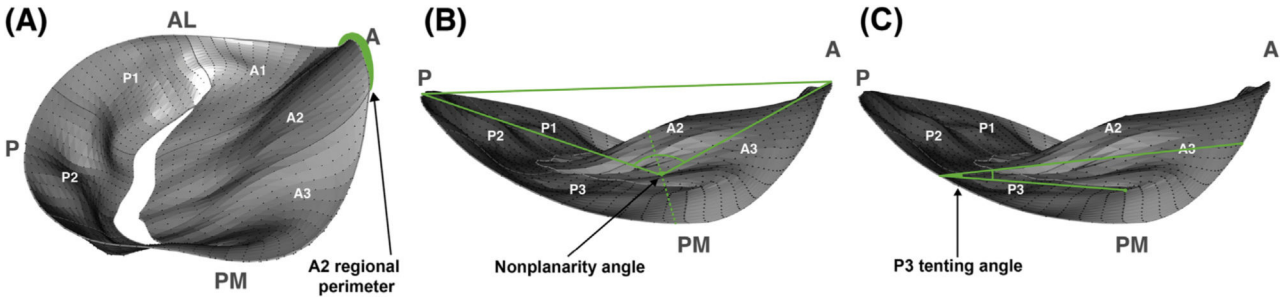

Fig 4.

Annotated illustrations of the three-dimensional reconstructions previously presented, clearly labeling (A) A2 regional perimeter, (B) nonplanarity angle, and (C) P3 tenting angle. (A = anterior; AL = anterolateral; P = posterior; PM = posteromedial.)

Table 1.

Measurement Definitions

Measurement	Definition
Diameter	Cartesian distance between two points
Tenting height	Maximum vertical displacement between anteroposterior plane and any valvular point
Perimeter	Cartesian distance through annular points
Leaflet area	Sum of areas of surface mesh triangles
Commissure width	Point-to-point Cartesian displacement across commissure
Commissure path length	Cartesian distance through all commissural points
Tenting volume	Sum of each product of the surface mesh triangle area projection on x-y plane and average displacement of triangular corners from interpolated annular surface
Nonplanarity angle	Angle between anterior high point (aortic insertion) and posterior high point that is subtended at the anterolateral-posteromedial diameter
Tenting angle	Angle between mid scallop annular point, mid opposite scallop annular point, and commissural intersection in between

Table 2.

Demographic Data for Ischemic Mitral Regurgitation Group and Control Group

Variable	IMR (n = 66)	Control (n = 10)
Sex		
Male	39	9
Female	27	1
Age, years, mean ± SD	68.74 ± 9.86	61.90 ± 10.22
Body mass index, kg/m^2, mean ± SD	30.44 ± 6.23	27.23 ± 4.10
Procedure		
Repair	54	0
Replacement	2	0
Other	10	10
Ejection fraction prebypass, %, median	40–45	50–55

IMR = ischemic mitral regurgitation.

Table 3.

Comparisons Between Ischemic Mitral Regurgitation Group and Control Group at Mid Systole

	IMR Group		Control Group		
Measurement	**Mean**	**SD**	**Mean**	**SD**	***p* Value**
AP diameter, mm	32.398	4.936	30.015	2.363	0.0210[a]
AL-PM diameter, mm	35.664	4.975	35.261	2.406	0.6844
Tenting height, mm	9.369	2.169	8.307	1.636	0.0891
P1 regional perimeter, mm	19.576	3.157	19.835	3.114	0.8107
P2 regional perimeter, mm	21.341	3.456	21.787	3.460	0.7105
P3 regional perimeter, mm	20.194	3.083	20.900	3.543	0.5626
Posterior perimeter, mm	61.111	9.492	62.522	9.664	0.6740
A1 regional perimeter, mm	20.075	3.539	18.670	1.913	0.0740
A2 regional perimeter, mm	11.149	2.007	9.798	1.065	0.0041[a]
A3 regional perimeter, mm	21.209	4.136	19.664	2.413	0.1091
Anterior perimeter, mm	52.433	8.791	48.132	4.102	0.0176[a]
Total perimeter, mm	113.544	15.416	110.655	7.983	0.3705
P1 regional leaflet area, mm2	154.207	48.073	136.997	41.910	0.2572
P2 regional leaflet area, mm2	237.035	78.467	216.000	82.173	0.4631
P3 regional leaflet area, mm2	157.709	60.205	155.306	49.938	0.8925
Posterior leaflet area, mm^2	548.950	179.190	508.304	165.200	0.4867
A1 regional leaflet area, mm2	160.486	47.142	132.316	25.248	0.0097[a]
A2 regional leaflet area, mm2	272.597	83.719	242.960	52.767	0.1493
A3 regional leaflet area, mm2	175.544	60.801	147.937	26.060	0.0196[a]
Anterior leaflet area, mm^2	608.627	178.557	523.214	90.463	0.0272[a]
Total leaflet area, mm^2	1,157.577	326.740	1,031.517	211.037	0.1247
Commissure width, mm	26.312	3.920	26.597	3.195	0.8032
Commissure path length, mm	36.422	6.579	34.912	5.385	0.4370
P1 regional tenting volume, mm3	263.220	203.515	215.843	126.468	0.3294
P2 regional tenting volume, mm3	463.010	478.014	472.649	326.301	0.9364

Ann Thorac Surg. Author manuscript; available in PMC 2019 August 07.

	IMR Group		Control Group		
Measurement	**Mean**	**SD**	**Mean**	**SD**	***p* Value**
P3 regional tenting volume, mm3	213.345	209.152	264.493	176.082	0.4193
Posterior tenting volume, mm^3	939.575	835.136	952.985	588.992	0.9506
A1 regional tenting volume, mm3	485.685	325.199	362.747	166.336	0.0767
A2 regional tenting volume, mm3	1,120.443	743.831	881.957	582.353	0.2658
A3 regional tenting volume, mm3	467.258	400.140	278.109	173.805	0.0163[a]
Anterior tenting volume, mm^3	2,073.386	1,366.984	1,522.813	862.615	0.1042
Total tenting volume, mm^3	3,012.961	2,038.754	2,475.798	1,388.260	0.3043
Nonplanarity angle, degrees	147.985	11.198	140.720	9.467	0.0459[a]
P1 tenting angle, degrees	40.196	8.380	37.040	8.010	0.2705
P2 tenting angle, degrees	36.710	14.060	33.071	11.295	0.3752
P3 tenting angle, degrees	44.354	7.818	40.461	4.767	0.0435[a]
A1 tenting angle, degrees	27.627	6.764	25.216	6.273	0.2836
A2 tenting angle, degrees	18.881	7.677	17.720	5.011	0.5380
A3 tenting angle, degrees	26.948	6.582	27.828	6.079	0.6802

[a]Indicates statistical significance at 0.05 level.

AL-PM = anterolateral-posteromedial; AP = anteroposterior; IMR = ischemic mitral regurgitation.

Table 4.

Multiple Logistic Regression Model for Predicting Incidence of Ischemic Mitral Regurgitation

Predictor	Coefficient	SE	z-Value	*p* Value	OR	95% CI Lower Bound	95% CI Upper Bound
(Intercept)	−15.033	6.337	−2.372	0.018	2.96E–07	2.90E–13	0.032
A2 regional perimeter, mm	0.447	0.244	1.834	0.067	1.564	1.010	2.674
Nonplanarity angle, degrees	0.058	0.033	1.757	0.079	1.059	0.994	1.134
P3 tenting angle, degrees	0.094	0.063	1.485	0.138	1.098	0.981	1.263

CI = confidence interval; OR = odds ratio.